WEP Warwick Evans Publishing

Transactions on Engineering and Technology Research
ISSN: 2960-1797, eISSN: 2960-2246 | Volume 6
MECEME 2026

Research on Enhancing the Resilience of Integrated Energy Systems Using Energy Routers

Chen Li *

College of Energy and Power Engineering, Changsha University of Science & Technology, Changsha, China

* Corresponding Author Email: 17749677387@163.com

Abstract. To address the vulnerability of Integrated Energy Systems (IES) to disruptions and enhance their resilience, this study employs an approach integrating Energy Routers (ER) into IES. The study minimizes total cost as the objective function and defines Expected Energy Not Supplied (EENS) as the core resilience metric. Focusing primarily on power systems and electrical loads, it employs randomly generated scenarios to compare traditional Business-As-Usual (BAU) operation with the innovative ER-integrated mode, analyzing metric variations across modes. Optimization model results show EENS reduced by 19.02% and total cost decreased by 18.94%. Furthermore, simulation results demonstrate that ER integration positively impacts metrics such as total load curtailment reduction and generator ramping capacity. This validates ER's crucial role in resilience enhancement and confirms the proposed methodology's feasibility and effectiveness.

Keywords: Integrated Energy System; Energy Router; Resilience Enhancement; Expected Energy Not Supplied; Multi-Scenario Comparison.

1. Introduction

As global climate change intensifies, extreme weather events such as typhoons, ice storms, and heatwaves occur with increasing frequency, posing unprecedented threats to the stable operation of power system infrastructure. Against this backdrop, the resilience of integrated energy systems—defined as their capacity to anticipate, withstand, adapt to, and rapidly recover from failures [1-3]—has become a focal point for both academic and industrial communities worldwide.

In recent years, significant progress has been made in enhancing the resilience of integrated energy systems. Yin et al. [4] proposes that resilience control measures can be categorized into preemptive preventive controls, corrective controls during incidents, and post-incident recovery controls. Huang et al. [5] proposed a high-temporal-resolution (hourly) quantitative assessment method for evaluating energy system resilience to support resilience enhancement. Chen et al. [6] introduced a comprehensive vulnerability identification approach for integrated energy systems that simultaneously considers operational risks and resilience to address threats to stable system operation posed by random disturbances. Jiang et al. [7] proposes an operational resilience assessment method for integrated energy systems based on arbitrary polynomial chaotic expansion under primary-aftershock impacts to mitigate negative effects of aftershocks. Zhou et al. [8] proposes a method for enhancing the resilience of hybrid AC/DC distribution networks by considering line reinforcement and energy storage resource allocation, offering valuable insights. However, existing research has primarily focused on static coupling analysis of multi-energy systems, failing to fully explore the synergistic enhancement potential of dynamic multi-energy flow coordination and flexible network topology reconfiguration for system resilience. Particularly during extreme events, energy subsystems remain coupled through traditional mechanical switching mechanisms, exhibiting slow response times and limited reconfiguration capabilities. This severely constrains the full realization of multi-energy synergy benefits.

As a core component of the energy internet, the introduction of energy routers provides a breakthrough solution to the aforementioned challenges. Sun et al. [9] provides an overview of multiple types of ERs, offering guidance for selecting ERs. Qiu et al. [10] proposes that ERs can

flexibly regulate grid power flows, rapidly control port power in real time, ensure mutual power balancing across interconnected grids, isolate faults, and enable flexible power redirection, thereby significantly enhancing distribution resilience. Li et al. [11] highlights that ERs offer advantages in information transmission, energy conversion, and portable access to diverse energy forms such as distributed energy sources and loads. Xu et al. [12] indicates that ERs are intelligent agents integrating computing, communication, precise control, remote coordination, and autonomy within the information-energy interconnection. The above literature demonstrates ER's potential to play a vital role in energy systems. Nevertheless, deeply integrating ER into the resilience optimization framework of IES faces several critical challenges: First, there is a lack of models for enhancing the resilience of integrated energy systems using ER. Second, methods for comprehensively validating the effectiveness of system resilience enhancement across multiple scenarios are insufficient. Third, the economic viability of such approaches has yet to be effectively demonstrated.

To address these challenges, this paper proposes a collaborative resilience enhancement strategy for IES based on ER. The research encompasses: constructing an optimization model for IES that accounts for fault scenarios; comparing performance metrics between BAU and advanced ER-integrated modes under fault conditions; defining a core resilience metric for enhancement evaluation; and quantitatively assessing the system resilience and economic benefits of ER while analyzing the strategy's engineering feasibility.

2. The Models and Methods

2.1. The System Architecture

The IES studied in this paper comprises the following primary components: conventional power generation units, renewable energy sources, battery energy storage systems, ER (multi-device parallel connection), electrical loads, and thermal loads. Shafiei et al. [13] introduced a multi-objective optimization model. The designed system integrates renewable energy and energy storage technologies. Ma et al. [14] proposes a coordinated configuration framework for soft open points and energy storage systems within integrated multi-energy port systems to address threats to the stability and resilience of port power systems posed by extreme weather events, emphasizing the role of energy storage systems. Therefore, this study incorporates these elements as well, enabling them to function effectively. Positioned centrally, the ER connects to each component, facilitating easy integration of new energy equipment and loads. Operational failures in individual subcomponents do not affect the operation of others. The system architecture is shown in Figure 1.

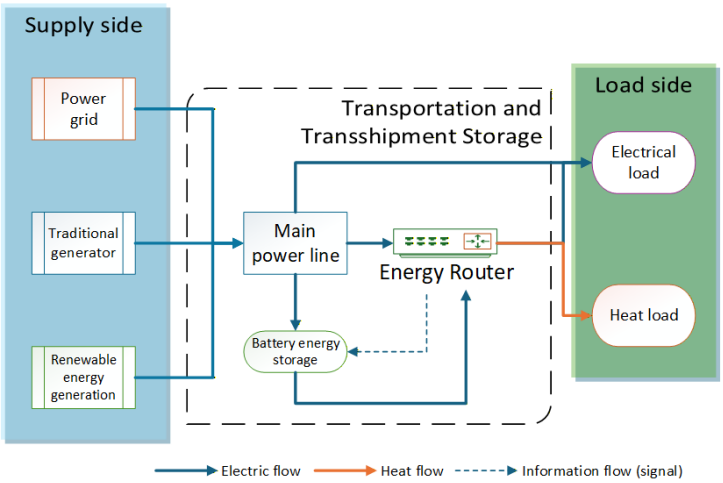

Figure 1. Comprehensive energy system architecture diagram

In power systems, the ER is a critical technological device within smart grids that leverages advanced computing and communication technologies to achieve efficient power distribution and dispatch [15]. Within this integrated energy system, the ER serves as a key flexible component, requiring the ability

to perform flexible conversion between different energy forms and power regulation to enhance system resilience. The integrated energy system model developed in this study is suitable for simplified research on regional-level energy systems, such as typical scenarios like industrial parks.

2.2. Mathematical Models and Methods

The objective function of the optimization problem is to minimize the total operating cost, comprising generation costs and load curtailment penalties:

$$min \sum_{t=1}^{T} \left(C^{gen} \cdot P_t^{gen} + C^{shed} \cdot \left(L_t^{elec,shed} + L_t^{therm,shed} \right) \right) \tag{1}$$

In the formula: C^{gen} represents the power generation cost coefficient, P_t^{gen} denotes the generator output at time t, C^{shed} represents the load reduction penalty coefficient, $L_t^{elec,shed}$ denotes the electricity load reduction at time t, $L_t^{therm,shed}$ denotes the heat load reduction at time t.

Define EENS as the core resilience indicator.

$$EENS = \sum_{s=1}^{S} p_s \cdot \sum_{t=1}^{T} \left(P_{s,t}^{shed,e} + P_{s,t}^{shed,h} \right) \tag{2}$$

In the formula: p_s denotes the probability of scenario s occurring; $P_{s,t}^{shed,e}$ represents the electric power deficit in scenario s at time t; $P_{s,t}^{shed,h}$ denotes the thermal power deficit in scenario s at time t. EENS, as a core resilience metric, not only effectively highlights the differences between the two models but also provides foundational support for subsequent economic analysis.This study includes the following constraints:

(1) Power balance constraint

$$P_t^{gen} + P_t^{ren} + P_t^{dis} - P_t^{ch} + \eta_{ER} \cdot P_t^{ER} = L_t^{e} - P_t^{shed,e} \tag{3}$$

In the equation: P_t^{ren} represents the power generation capacity of renewable energy at time t; P_t^{dis} represents the power discharge capacity of energy storage at time t; P_t^{ch} represents the power charging capacity of energy storage at time t; η_{ER} represents the comprehensive efficiency coefficient of the energy router; P_t^{ER} denotes the bidirectional flow characteristic of energy, which can be positive or negative; L_t^{e} represents the electricity load demand at time t; $P_t^{shed,e}$ represents the electricity load reduction at time t.

This constraint ensures that the amount of electricity injected (left side) equals the amount of electricity consumed (right side). When a power deficit occurs in the system, real-time balance is maintained by adjusting generator output, energy storage charging/discharging, energy router power, and necessary load shedding.

(2) Power balance constraint

$$P_t^{shed,h} \leq L_t^{h} \tag{4}$$

In the formula: $P_t^{shed,h}$ denotes the shedding amount of thermal load at time t, and L_t^{h} denotes the thermal load demand at time t.

Thermal balance constraints are relatively simplified, primarily limiting the scope of heat load reduction and reflecting the unique characteristics of thermal systems. Unlike electrical systems, thermal systems possess significant thermal capacity due to components such as pipelines and buildings, enabling tolerance for short-term imbalances. This constraint ensures heat load reduction

remains within reasonable limits, thereby safeguarding heating quality while providing operational flexibility for the system.

(3) Energy storage system constraints

$$\begin{cases} SOC_t = SOC_{t-1} + P_t^{ch} - P_t^{dis} \\ SOC^{min} \le SOC_t \le SOC^{max} \\ 0 \le P_t^{ch} \le P_{ch}^{max} \\ 0 \le P_t^{dis} \le P_{dis}^{max} \end{cases} \tag{5}$$

In the equation: SOC_t denotes the state of charge at time t, SOC^{min} represents the minimum state of charge, SOC^{max} denotes the maximum state of charge, P_{ch}^{max} indicates the maximum charging power, and P_{dis}^{max} denotes the maximum discharging power.

Energy storage systems optimize system operation through peak shaving and valley filling. They charge during low-load periods and discharge during peak load periods or outages, enhancing system economics and reliability. Four constraints collectively ensure energy storage operates within safe parameters.

(4) ER constraint

$$-P_{ER}^{max} \le P_t^{ER} \le P_{ER}^{max} \tag{6}$$

In the equation: P_t^{ER} denotes the transmission power of the ER at time t, and P_{ER}^{max} denotes the maximum transmission power of the ER.

As a coupling device within multi-energy systems, the ER enables flexible conversion and power regulation between different energy forms. This constraint ensures the ER operates within the safe working range of the equipment while providing the system with a critical flexibility resource.

(5) Generator operating constraints

$$\begin{cases} P_{gen}^{min} \le P_t^{gen} \le P_{gen}^{max} \\ \left| P_t^{gen} - P_{t-1}^{gen} \right| \le R^{up} \\ \left| P_{t-1}^{gen} - P_t^{gen} \right| \le R^{down} \end{cases} \tag{7}$$

In the formula: P_{gen}^{min} denotes the minimum technical output of the generator, P_{gen}^{max} denotes the maximum technical output of the generator, R^{up} denotes the ramp-up rate, and R^{down} denotes the ramp-down rate.

Generator operating constraints ensure power generation equipment operates under safe conditions. Output upper and lower limits define the stable operating range for generators, while ramp rate constraints guarantee smooth power changes, preventing equipment damage or system instability caused by sudden power fluctuations.

The aforementioned constraints collectively form the complete operational framework of the IES. Balance constraints ensure real-time matching of energy supply and demand, equipment constraints define the operational boundaries of individual devices, and energy storage constraints describe the spatiotemporal transfer characteristics of energy. All constraints are mutually coupled and coordinated through collaborative solution-seeking to achieve overall optimal system operation. During fault conditions, the interactions among these constraints become more complex. When generator capacity is constrained, the system maintains safe and stable operation by mobilizing

flexible resources such as energy storage and ER, and by shedding load when necessary. This mechanism of multi-constraint collaborative optimization is a key manifestation of the resilience inherent in IES.

The conversion efficiency modeling of ERs and their component models can be represented in matrix form [16-17]. The matrix-based ER model adopted in this study is as follows:

$$\begin{bmatrix} 1 & 0 & 0 & 0 & \eta_{ER} & -1 & 0 \\ 0 & 0 & 0 & 0 & \eta_{ER} & 0 & 1 \\ 0 & 0 & 0 & 0 & 1 & 0 & 0 \\ 0 & 0 & 0 & 0 & -1 & 0 & 0 \end{bmatrix} \cdot \begin{bmatrix} P_t^{gen} \\ P_t^{ren} \\ P_t^{dis} \\ P_t^{ch} \\ P_t^{ER} \\ L_t^e \\ L_t^h \end{bmatrix} = \begin{bmatrix} -P_t^{shed,e} \\ L_t^h - P_t^{shed,h} \\ P_{ER}^{max} \\ P_{ER}^{max} \end{bmatrix} \tag{8}$$

This integrated model describes the power balance, energy conversion, capacity constraints, and efficiency characteristics of ER, providing a mathematical foundation for the optimized operation of IES.

3. Case Analysis

3.1. Basic Parameter Settings and Scene Generation

The parameter design adopted in this study is based on the concept of stress testing, aiming to construct a high-pressure scenario capable of fully exposing system vulnerabilities and effectively evaluating resilience enhancement measures. The comprehensive electricity load and comprehensive heat load data for a Beijing district from Reference [18] were used to design the baseline electricity load and heat load for this study. Since this research primarily focuses on electricity load, the proportions of electricity and heat load data in the reference were adjusted accordingly. The baseline electricity load corresponds to the typical power consumption scale of a medium-sized urban area or large industrial park, with an electricity-to-heat load ratio of approximately 1.33:1, consistent with typical regional energy system configurations. Parameters such as power ratings were designed based on typical efficiencies achievable with current power electronics and heat exchange technologies. Drawing upon the economic component of the planning model in Reference [19], this study primarily considers generation costs and load curtailment costs. Cost parameters were designed by referencing typical ranges of electricity market clearing prices and drawing from statistical research on economic losses from power outages. Specific parameters are shown in Table 1.

Table 1. Parameters for high-voltage operation scenarios

Parameter name	Parameter value	Unit
Number of time cycles	12	Hour
Basic electrical load	80	MW
Base heat load	60	MW
Maximum output of the generator	80	MW
Minimum output of the generator	8	MW
Generation cost	50	$/MWh
ER maximum transmit power	8	MW
ER efficiency	0.98	-
Battery capacity	50	MWh
Maximum charge/discharge power	20	MW
Failure start time	5	Hour
Duration of the failure	4	Hour

Load-cutting penalty coefficient	10000	\$/MWh

On the composition of multi-scene sets: generate two representative operational scenarios for comparative analysis to reduce single-instance randomness and enhance credibility. Each scenario has a 50% probability and integrates multiple stresses including load fluctuations, renewable energy output uncertainty [20], and equipment failures. Both BAU and integrated ER modes are run for each scenario, enabling a thorough comparison that demonstrates the optimization performance of ER. Next is the design of electrical load and thermal load scenarios.

$$L_t^e = L_{base}^e \times \left(0.8 + 0.4 \times \xi_t\right) \tag{9}$$

In the equation: L_{base}^e represents the base electrical load, and ξ_t denotes a uniformly distributed random variable with a range of 0 to 1.

Based on the fundamental parameters of the scenario, the electrical load fluctuation range is 64-96 MW, capable of simulating both nighttime loads and peak loads or sudden electricity demands, with a fluctuation amplitude of ±20%. This effectively simulates the uncertainty of load-side response. Similarly, the thermal load fluctuation range is determined to be 48-72 MW. This load is generated independently and randomly from the electrical load, establishing an indirect coupling relationship through ER. The renewable energy output scenario design is employing a differentiated generation strategy for day and night periods, daytime operations prioritize photovoltaic power generation with an output range of 10–20 MW, simulating cloud movement and atmospheric condition variations; nighttime operations prioritize wind power generation with an output range of 2–5 MW. The failure commenced at the 5th hour and persisted for 4 hours, during which the system's power generation capacity dropped to 10%, simulating an extreme generator failure. This extreme stress was applied during a vulnerable period to test the system's resilience under severe faults. As this study primarily focuses on power systems and electrical loads, its impact on thermal systems and thermal load supply is minimal and will not be explored in detail. Moreover, the power grid is operating normally, with its electricity primarily supplied to the load side via the main power lines, while the portion fed into the ER can be considered negligible. In this study, the power grid does not serve as the primary power generation unit.

3.2. Results Analysis

Through case simulations, the system operated across multiple scenarios and synthesized the results, ultimately yielding the following outcomes:

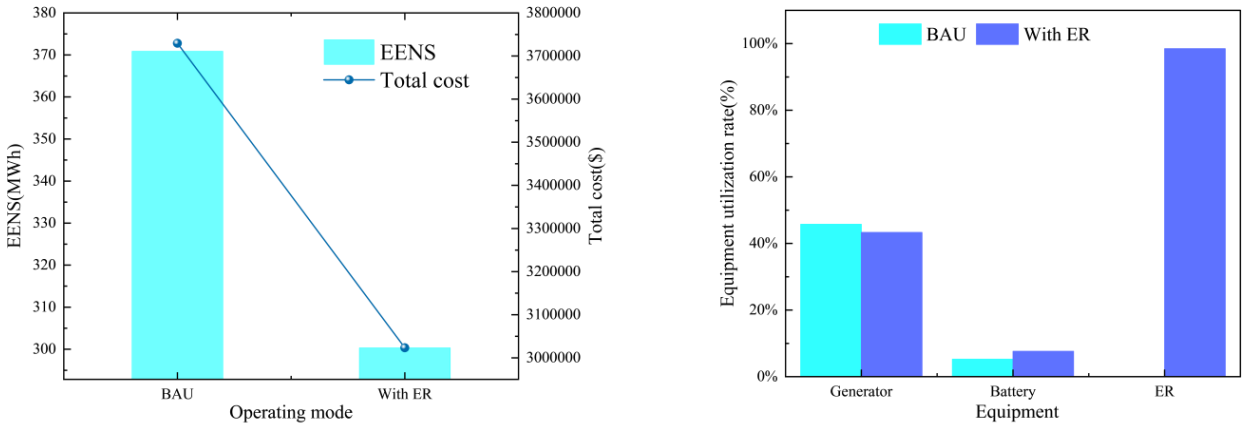

(a) EENS and total costs (b) Equipment utilization rates

Figure 2. Comprehensive comparison of multiple scenarios and modes across various metrics

Table 2. Detailed breakdown of total cost

Cost type	BAU model （$）	ER model ($)	Change amount ($)	Change ratio
Generation cost	20797.25	20013.25	784.00	3.77%
Load penalty cost	3708866.55	3003266.55	705600.00	19.02%

As shown in Figure 2(a), under comprehensive multi-scenario conditions, the ER mode achieved an EENS value of 300.33 MWh. Compared to the 370.89 MWh achieved by the BAU mode, the total EENS decreased by 19.02%, representing a significant improvement. This demonstrates that the ER effectively enhances system power supply reliability under fault conditions, playing a critical role during the system's most vulnerable periods. The changes in core metrics reflect an effective enhancement of the integrated energy system's resilience. Economically, the total cost under the ER mode was $3,023,279.80, representing an 18.94% reduction compared to the conventional mode's $3,729,663.80. The cost breakdown in Table 2 shows that the ER mode primarily achieved this reduction by minimizing load penalty costs. This demonstrates the economic viability of the proposed solution.

The data in Figure 2(b) indicates that under the ER mode, the utilization rate of the generator set decreased by approximately 2.45%, while the utilization rate of the battery bank increased by about 2.36%. This demonstrates that the integration of ER reduces the system's reliance on generator output, enabling the effective utilization of energy storage batteries. This phenomenon reflects both the enhanced multi-energy utilization efficiency achieved by ER within the system and the strengthened resilience of the system.

Table 3. Scenario 1: comparison of key metrics

Key metrics	BAU	With ER
Maximum electrical load reduction/(MW)	72.37	64.53
Average generator output/(MW)	36.11	34.80
Average battery SOC during failure period/(MWh)	10.12	10.77
Total Load Reduction During failure period/(MW)	249.14	217.78

Table 4. Scenario 2: comparison of key metrics

Key metrics	BAU	With ER
Maximum electrical load reduction/(MW)	63.49	55.65
Average generator output/(MW)	33.22	31.91
Average battery SOC during failure period/(MWh)	10.10	10.76
Total Load Reduction During failure period/(MW)	230.75	199.39

Based on the data in Tables 3 and 4, both scenarios exhibit a downward trend in maximum load reduction, average generator output power, and total load reduction during faults following ER integration. The average battery SOC during failure period shows a slight increase. This indicates that the energy recovery system plays a positive role in both scenarios, effectively mitigating the inherent randomness of the single-scenario approach. Given that the operational results of the two scenarios are largely comparable, to avoid redundant analysis, this paper will use Scenario 1 as the basis for further analysis.

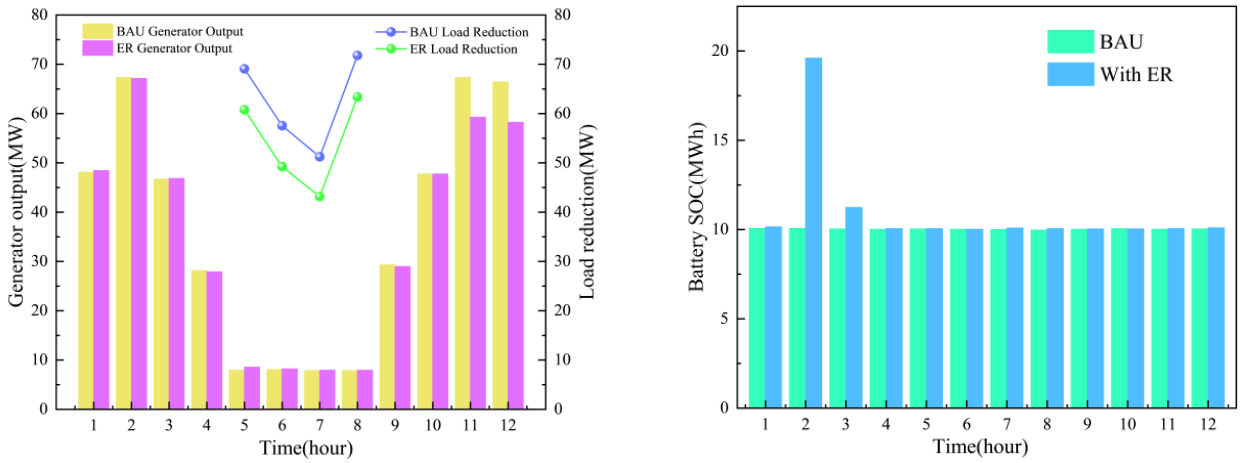

(a) Generator output at each time point and load reduction during the outage period

(b) Battery SOC

Figure 3. Scenario 1: comparison of key metrics

Figure 3(a) shows that the output of the generator in the two modes was similar during the initial phase. However, after the fault, the output level in ER mode decreased. This indicates that ER mode reduces the generator's ramping requirements, achieving the goal of supplying power to the load side. It meets the same energy demand of the load side under BAU mode with lower output power, thereby minimizing generator energy consumption. Additionally, the ER mode significantly reduces the total load shedding during outages, enabling substantial reductions in system restoration time and enhancing resilience. Figure 3(b) data indicates that in ER mode, the battery employs scheduled preventive charging to address sudden faults, effectively extending the average SOC range during outages. This preventive charging mechanism enables the energy storage system to maintain continuous power supply to the load side during faults, ensuring no significant drop in power delivery to the load side during fault events.

4. Conclusions and Outlook

This study proposes a method to enhance the resilience of IES by incorporating ER. First, an ER-based IES model is constructed, followed by comparative analysis across multiple scenarios and modes. Through systematic analysis, the following key conclusions are drawn: First, the ER significantly enhances the resilience of IES under extreme fault conditions. After ER integration, the EENS decreases by 19.02%, and the total load curtailment reduction during faults reaches approximately 13%. Second, under high-voltage multi-scenario conditions, the ER mode achieves significant cost savings compared to the BAU mode, demonstrating proven economic viability. These savings primarily stem from reduced load curtailment penalty costs. Annual cost savings reached $706,384, representing a 18.94% reduction. Furthermore, the ER reduced average generator output and activated energy storage systems, demonstrating that beyond direct economic benefits, it delivers multiple values including enhanced equipment reliability and improved environmental energy consumption. Simulation results validate the feasibility of the resilience enhancement approach proposed in this study. Multi-energy flows can be efficiently converted within the ER, enabling multi-energy complementarity.

Based on this study, the following future development directions are proposed: First, expand the model to incorporate more extreme event scenarios (such as cascading failures and cyberattacks) while systematically considering and analyzing thermal systems. Subsequently, technical details should be refined, including: refining the modeling of ER investment costs, evaluating cost differences among various technical solutions, and exploring more economically viable alternatives. Second, advance strategy optimization research by studying coordinated optimization strategies for multiple ERs and exploring distributed deployment schemes to enhance optimization efficiency.

Concurrently, investigate market mechanisms, such as examining commercial operation models and value realization mechanisms for ERs within market environments. Research may also focus on the role of energy storage devices like batteries in enhancing system resilience and improving efficiency. Finally, conduct empirical studies to validate the accuracy of theoretical models through engineering practice.

References

[1] Monie S W, Gustafsson M, Önnered S, et al. Renewable and integrated energy system resilience–A review and generic resilience index[J]. Renewable and Sustainable Energy Reviews, 2025, 215: 115554.

[2] Zhang Rufeng, Li Xue, Jiang Tao, Chen Houhe. A review of resilience assessment and enhancement for urban integrated energy systems[J]. Journal of Global Energy Interconnection, 2021, 4 (02): 122-132.

[3] Kang S, Peng B, Wang Y. Research progress, hot spot evolution and future directions of energy system resilience: A bibliometric overview[J]. Energy Reports, 2025, 14: 3451-3467.

[4] Yin Jijun, Xia Qing. Conceptual Design and Exploration of Multi-source Integrated High-resilience Power Grids in the Energy Internet Framework [J]. Proceedings of the CSEE, 2021, 41 (02): 486-497.

[5] Huang Jingzhi, Xiao Ning, Huang Xianan, Lin Changzhui, Hu Zhenda, Liu Lin, Wu Nianyuan, Zi Zhengyu, Lin Jian, Xie Shan, Jing Rui, Zhao Yingru. Electro-hydrogen coupled integrated energy systems: resilience quantification and multi-objective optimization[J]. Clean Coal Technology, 2024, 30 (12): 147-160.

[6] Chen Lijuan, Liu Li, Zhou Chang, Xu Xiaohui. Identification of vulnerabilities in integrated energy systems considering operational risks and resilience [J]. Automation of Electric Power Systems, 2022, 46 (06): 48-57.

[7] Jiang Tao, Qiu Yuxin, Liu Zeyu, Li Xue, Hou Kai, Jia Hongjie. A resilience assessment method for integrated energy system operations in response to main aftershocks [J]. Proceedings of the CSEE, 1-13.

[8] Zhou Shichao, Liu Xiaolin, Xiong Zhan, Wang Xu, Jiang Chuanwen, Zhang Shenxi. Reinforcement and Energy Storage Configuration Strategy for AC/DC Distribution Networks Considering Resilience Enhancement. [J]. Journal of Shanghai Jiaotong University(Science), 2021, 55 (12): 1619-1630.

[9] Sun Qiuyue, Xing Rongda, Shen Qianxiang, Sun Zhen'ao. A review of multi-type energy routers [J]. Journal of Northeastern University(Natural Science), 2025, 46 (07): 11-21.

[10] Qiu Shushan, Chen Jinfan, Mao Chengxiong, Ma Chunyan, Liu Zhe, Wang Dan. Coordinated Dynamic Optimization of AC-DC Interconnected Distribution Networks with Energy Storage Routers[J]. High Voltage Engineering, 2023, 49 (01): 147-158.

[11] Li Zezheng, Ye Peng, Zhang Zhengbin, Zhang Mingli. Research on energy management of energy routers in integrated energy systems [J]. Northeast Electric Power Technology, 2023, 44 (12): 68-74.

[12] Xu Xiaohui, Zhang Maojie, Pan Junfeng, Xu Chenghu, Zhang Hao. Particle Swarm Optimization Algorithm for Energy Dispatch in Multi-Port Energy Routers: Source-Grid-Load-Storage Integration [J]. Journal of Naval University of Engineering, 2024, 36 (02): 19-24.

[13] Shafiei K, Seifi A, Hagh M T. A novel multi-objective optimization approach for resilience enhancement considering integrated energy systems with renewable energy, energy storage, energy sharing, and demand-side management[J]. Journal of Energy Storage, 2025, 115: 115966.

[14] Ma W, Tang D, Dong M, et al. Coordinated robust configuration of soft open point and energy storage systems for resilience enhancement of integrated multi-energy system at ports[J]. Applied Energy, 2025, 401: 126644.

[15] He Mingfeng, Ye Xujing, Bao Weihong, Yang Jian, Wang Ke, Chen Jian, Xu Chong, Fu Xianfeng, Li Zhi. Research on source-grid-load-storage coordination based on power energy routers [J]. Electrical Equipment and Economy, 2024, (05): 213-215.

[16] Zhang Zhengbin, Ye Peng, Zhang Na, Cheng Mengzeng. Joint optimization dispatch of generation, load, and storage in microgrids based on energy routers [J]. Hebei Electric Power, 2022, 41 (03): 30-36.

[17] He Jinsong, Zhang Yu, Chen Yushu, Hou Yanpeng, Li Zezheng, Wang Huan. Multi-timescale low-carbon dispatch strategy for industrial parks based on energy routers [J]. Renewable Energy Resources, 2024, 42 (09): 1253-1261.

[18] Weng Sijuan, Cui Yue. Analysis of energy system proportions in a regional energy station in Beijing [J]. Heating Ventilating & Air Conditioning, 2020, 50 (05): 75-78.

[19] Lv H, Wu Q, Ren H, et al. A two-stage decision-making approach for optimal design and operation of integrated energy systems considering multiple uncertainties and diverse resilience needs[J]. Energy, 2024, 305: 132375.

[20] Chen Y, Yang S, Wang Y, et al. Dual time-scale operation control strategies for high-altitude integrated energy systems considering source-load uncertainty[J]. International Journal of Electrical Power & Energy Systems, 2025, 172: 111147.